Using noise to determine cardiac restitution with memory

Shu Dai and James P. Keener

Phys. Rev. E **85**, 061902 — Published 1 June 2012

DOI: 10.1103/PhysRevE.85.061902

Using noise to determine cardiac restitution with memory

Shu Dai [1] and James P. Keener [2]

[1]Mathematical Biosciences Institute,

The Ohio State University, Columbus, OH 43210 USA

[2]Department of Mathematics,

The University of Utah, Salt Lake City, UT 84112 USA

Abstract

Variation in cardiac pacing cycles as seen, for example, in heart rate variability, has been observed for decades. Contemporarily, various mathematical models have been constructed to investigate the electrical activity of paced cardiac cells. Yet there has not been a study of these cardiac models when there is variation in the pacing cycles such as noise. In this paper, we present a method that uses the stochasticity of pacing cycles to determine approximate models of the dynamics of cardiac cells, and use these models to detect bifurcations to alternans.

1 Introduction

The mathematical study of the dynamics of electrical activity of cardiac cells has a long history. One of the primary problems is to determine the response of a cardiac cell to periodic stimuli, and to identify and characterize bifurcations in these behaviors. While detailed ionic models have been used extensively for this study [1, 2, 3, 4, 5], mapping models, pioneered by Nolasco et al. [6, 7], are introduced in the past decades to focus on the *restitution*, i.e. the dependence of and action potential durations (APD) on preceding diastolic interval (DI). In particular, period-doubling bifurcation occurs as the exterior stimuli pace sufficiently fast and alternation of APDs, which is called *alternans*, emerges, as illustrated in Figure 2. Recent mapping models involve memory variables in the restitution, which are often related to the intracellular ion (mostly calcium) concentrations in different compartments, to explain more complicated restitutions [8, 9, 10, 11,

12, 13]. The memories in those models are usually hidden and hard to be detected in experiments, hence it is difficult to reconstruct the model directly. The new method we will develop in this paper provides one way to approximate the restitution by an alternative form, using stochastic pacing cycles, and we assume only pacing cycles and APDs are detectable.

The simple mapping model proposed in [6] suggests that the preceding DI completely determined the APD, i.e.,

$$A_n = f(D_{n-1}), \tag{1.1}$$

for some restitution function f, where A_n and D_n represent the n^{th} APD and DI, respectively. With a fixed Basic Cycle Length (BCL) with $A_n + D_n = BCL \equiv \mu$, (1.1) becomes a simple 1-dimensional map. Typically, f is a non-decreasing function of D, so that there is a unique fixed point A^* which is an increasing function of μ. This is referred to as a 1:1 response. A period-doubling bifurcation (2:2 response) occurs if $f'(D^*)$ increases across 1 as μ decreases, where $D^* = \mu - A^*$, and alternans emerges as a long-short alternation of APD.

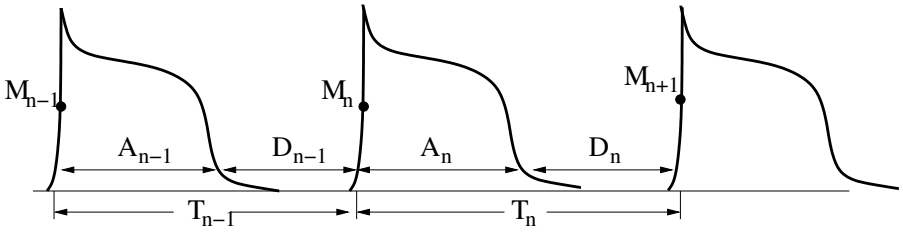

Figure 1: Illustration of the cycle lengths T_n, action potential duration A_n, diastolic interval D_n and memory variable M_n.

Memories are introduced recently for more complicated dynamics that are not explained by the simple 1-D maps. We can summarize the general form of a model involving J memory variables as

$$\begin{cases} A_n = f(D_{n-1}, M_n^{(1)}, M_n^{(2)}, \ldots, M_n^{(J)}), \\ M_n^{(i)} = g_i(A_{n-1}, M_{n-1}^{(i)}, T_{n-1}), \quad \text{for } i = 1, 2, \ldots, J, \\ D_n = T_n - A_n, \end{cases} \tag{1.2}$$

where A_n is the n^{th} APD; T_n is the time between n^{th} and $(n+1)^{st}$ exterior stimulus; D_n is the DI following A_n; and $M_n^{(i)}$ are the memory variables at the time that the n^{th} stimulus occurs. Figure 1 illustrates the variables in the model, with one memory variable shown.

A given series of stimulus intervals $\{T_n\}$ is called a pacing cycle protocol. For typical memory models, when T_n's are constant μ (S1 protocol), the system (1.2) has a fixed point $(A^*, M_*^{(1)}, M_*^{(2)}, \ldots, M_*^{(J)})$ if μ is sufficiently large. The fixed point may lose its stability through a period-doubling bifurcation to alternans when μ is below some critical value μ_c. The solid and dashed curves in Figure 2 illustrate a typical bifurcation diagram (only values of APD's are shown in the graph).

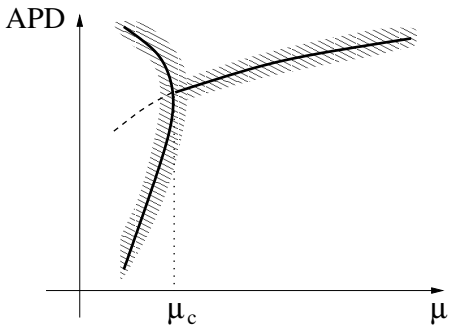

Figure 2: Typical bifurcation diagram for a cardiac mapping model with constant cycle length μ, where period doubling bifurcation occurs at $\mu = \mu_c$. The shadow region indicates the range of APD's when the cycle length has a small random fluctuation around μ.

In many situations, the pacing interval T_n's are nonconstant, i.e., there is variation in the times between consecutive stimuli. For example, in real hearts, heart rate variability is well known [20, 21, 22]. Figure 3 shows an example of a series of natural pacing cycles for a healthy human heart [23].

When the pacing intervals T_n's are nonconstant, in the long time run, we do not expect convergence to a fixed point or alternans. However, if the variation in T_n's is small enough, it may be that in the long run the APD's are located in a neighborhood of the fixed point or alternans, such as the shadow region shown in Figure 2. Thus, even in the presence of noise, there is some information about bifurcations to be gleaned from the APD's, but how much is not yet known.

In this paper we discuss the following question: Given a (random) sequence of pacing times T_n and the corresponding APD's A_n, to what extent can the restitution function f and the resulting bifurcation structure and dynamics be determined? To make initial progress, we assume that the data are generated by some mapping model of the form (1.2). Thus, we are provided with a series of T_n's and corresponding A_n's, however, the memory terms $M_n^{(i)}$ in (1.2) are hidden variables and cannot be detected. In what follows we develop a regression algorithm with which we are able to obtain an approximate equivalent form having dynamics similar to (1.2). Furthermore, since the data are generated by a known model, we have a check for how good our approximate restitution function and bifurcation structure are.

The organization of the paper is as the following. In Section 2, we introduce our ideas using a simple memory model proposed by Tolkacheva et al. [16]. In Section 3, we discuss a more general mapping model with one memory variable, using a model suggested by Fox et al. [15] as an example. In Section 4 we discuss the most general case of a mapping model with multiple memory variables, as in (1.2). Section 5 is the discussion, and Section 6 is the conclusion.

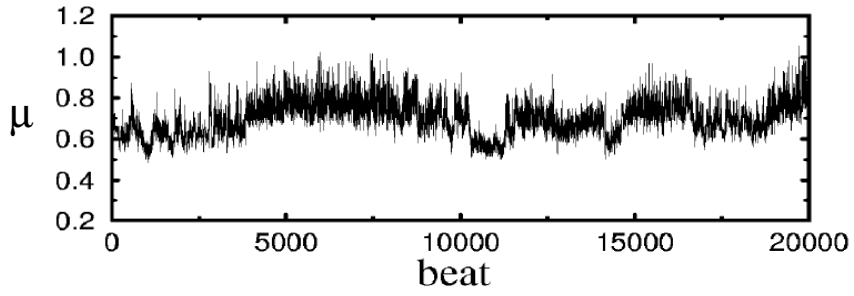

Figure 3: Sequence of interbeat intervals (in unit of second) for a healthy individual, L.A.N. Amaral et al., Computer Physics Communications 121-122(1999) 126-128.

2 Approximate Tolkacheva et al.'s Model

The mapping model proposed by Tolkacheva et al. [16] is in the form

$$A_n = f(D_{n-1}, A_{n-1}), \tag{2.1}$$

which is a special case of the general mapping model (1.2) with $J = 1$ and $M_n^{(1)} = A_{n-1}$. The details of the model are given in the appendix. If A^* is a fixed point when the pacing intervals are the constant μ, its stability is determined by the derivative

$$f' = \left.\frac{df}{dA}\right|_{A^*} = -\left.\frac{\partial f}{\partial D}\right|_{D^*} + \left.\frac{\partial f}{\partial A}\right|_{A^*},$$

where $D^* = \mu - A^*$.

Previous analysis has shown that in the 1:1 response case, one can estimate f' from experiments by the following process (for more details see [16]). First, for a given BCL μ, the fixed point A^* and associated D^* satisfy

$$A^* = f(D^*, A^*) = f(\mu - A^*, A^*),$$

and we record the fixed points A^* and associated D^* for different BCL's to obtain the *dynamic restitution curve* (RC). The slope of dynamic RC at a particular (A^*, D^*) that we are interested in is estimated by

$$S_{\rm dyn} = \frac{\partial A^*}{\partial D^*} = \frac{\partial f/\partial D_{n-1}|_{A_{n-1}=A*}}{1 - \partial f/\partial D_{n-1}|_{A_{n-1}=A*}}.$$

Then, we use the S1-S2 stimulus protocol: a long series of constant stimulus intervals, $\mu_{S1} = \mu$, followed by a single stimulus with a different interval μ_{S2}. The measured APD A_{S1S2} is given by

$$A_{S1S2} = f(D_{S1S2}, A^*),$$

where A^* is the fixed point corresponding to BCL $\mu_{S1} = \mu$ and $D_{S1S2} = \mu_{S2} - A^*$, and the *S1-S2 RC* is the plot of A_{S1S2} versus D_{S1S2}. The slope of S1-S2 RC at $D_* = \mu - A^*$ is given by

$$S_{\mathrm{S1S2}} = \left.\frac{dA_{S1S2}}{dD_{S1S2}}\right|_{D_{S1S2}=D^*} = \left.\frac{\partial f}{\partial D_{n-1}}\right|_{A_{n-1}=A^*}. \tag{2.2}$$

The two slopes S_{dyn} and S_{S1S2} can be estimated by finite difference method in experiments, and value of f' follows from the chain rule

$$f' = 1 - \left(1 + \frac{1}{S_{\mathrm{dyn}}}\right) S_{S1S2}. \tag{2.3}$$

The method we implement below to approximate f is to make the pacing cycles stochastic, which we call the "*stochastic protocol*". We show that we can approximate the dynamics of the mapping model (2.1) in an interval $[\mu_a, \mu_b]$ rather than simply at a single point as in (2.3). Furthermore, we can include cases when a period-two bifurcation occurs and alternans appears in the interval $[\mu_a, \mu_b]$.

We assume the pacing cycles T_n are randomly distributed in $[\mu_a, \mu_b]$, and the action potential durations A_n's are generated through (A.1) with a random initial value. We define $\bar{T}$ to be the sample mean of the cycles T_n, i.e.,

$$\bar{T} = \mathrm{mean}(T_n). \tag{2.4}$$

If the variation of the cycles, i.e., the range of the interval $\mu_b - \mu_a$, is small, we may regard all T_n's as perturbations of μ. For simplicity, we first consider the 1:1 response case. In the case of constant pacing with cycle μ, there is a stable fixed point A^*, such that

$$A^* = f(D^*, A^*), \tag{2.5}$$

where $D^* = \mu - A^*$. Since T_n's are perturbations of μ, we naturally assume all A_n's are small perturbations around A^*. The leading order approximation is

$$a_n \sim f_1 d_{n-1} + f_2 a_{n-1} = \widetilde{f}_1 a_{n-1} + \widetilde{f}_2 t_{n-1}, \tag{2.6}$$

where $a_n = A_n - A^*$, $d_n = D_n - D^*$, and f_1 and f_2 are the partial derivatives of f with respect to D_{n-1} and A_{n-1} at the fixed point, and $\widetilde{f}_1 = f_2 - f_1, \quad \widetilde{f}_2 = f_1$. We take the covariance of the equation (2.6) with a_n and t_n respectively to obtain two approximating equations,

$$\begin{cases} \langle a_n, t_{n-1}\rangle \sim \widetilde{f}_1 \langle a_{n-1}, t_{n-1}\rangle + \widetilde{f}_2 \langle t_{n-1}, t_{n-1}\rangle, \\ \langle a_n, a_{n-1}\rangle \sim \widetilde{f}_1 \langle a_{n-1}, a_{n-1}\rangle + \widetilde{f}_2 \langle t_{n-1}, a_{n-1}\rangle. \end{cases} \tag{2.7}$$

Then the derivatives $\widetilde{f}_1$ and $\widetilde{f}_2$ may determined directly by solving the above two-dimensional linear system.

The above process is equivalent to using simple linear regression to find the best least squares fit of the equations (2.6) with two unknown coefficients. The method of fitting data in a least squares sense has been applied widely in previous research [12, 24], in which some functional form of the restitution is proposed and unknown parameters are then determined by regression analysis, i.e., by minimizing the squared error of the fit.

Here we do not assume a particular form for the restitution function f, i.e., f is completely unknown. We extend the above case of a linear approximation (2.6) to higher orders, i.e., by considering the Taylor polynomial expansion of f. In general, we are looking for a polynomial $H_1^p(A_{n-1}, T_{n-1})$ of given order p in the following form,

$$A_n \sim H_1^p(A_{n-1}, T_{n-1}) = \sum_{0 \le \alpha+\beta \le p} f_{\alpha\beta}(A_{n-1} - \bar{A})^\alpha (T_{n-1} - \bar{T})^\beta, \tag{2.8}$$

which best fits the given data of T_n and A_n. Here $\bar{T}$ and $\bar{A}$ are the means of the pacing cycles T_n and APDs A_n respectively. The subscript 1 in H_1^p indicates that the restitution function $f(D_{n-1}, A_{n-1})$ depends only on the most recent previous beat. The unknown coefficients $f_{\alpha\beta}$ are to be determined. We note that $\bar{A}$ is not the fixed point solution A^* corresponding to $\bar{T}$, however, we can compute A^* from (2.8) once the coefficients are found.

To carry out this procedure for a specific example, we pick $N = 1000$ pseudo-random pacing cycles T_n, which are uniformly distributed[1] in the time interval $[\mu_a, \mu_b]$ with $\mu_a = 295$ms and $\mu_b = 305$ms. The theoretical bifurcation point $\mu_c \approx 301.40$ms is located in this interval. We record the series of corresponding APDs A_n generated through the original model (A.1). To mimic the measurement error of APDs in experiments, we add small noise to A_n, after the sequence is generated,

$$A_n \to A_n + \epsilon\xi_n, \tag{2.9}$$

where $\epsilon = 0.01$ms is the magnitude of error, and ξ_n's are independent identically distributed standard normal random variables. For convenience, we do not change the notation for A_n. We assume the error in measuring pacing cycles is negligible. The sequences of T_n and A_n are shown in Figure 4. We also plot a histogram of the APDs in Figure 4, from which we observe an apparent distribution involving alternans.

To obtain a period-doubling bifurcation from the approximating polynomial H_1^p, it is required that $p \ge 2$. We use linear regression to find the coefficients $f_{\alpha\beta}$ for each p of interest. Table 1 shows a statistical analysis for the case $p = 2$, for which there are 6 unknown coefficients $f_{\alpha\beta}$'s.

We repeat the above process for various values of order p using the same data set. After obtaining the coefficients $f_{\alpha\beta}$'s, we compare the approximate iterative function $H_1^p(A_{n-1}, T_{n-1})$ with the original model. In Figure 5 we show their bifurcation diagrams for $p = 2, 4, 5$ respectively. One can observe that with order $p = 5$, the dynamics of H_1^p are very close to the theoretical prediction.

[1]Uniform distribution is used as an example. In fact our approach does not depend on the distribution type of the pacing cycles. See the discussion in Section 5.

Coefficients	Estimate	Std. Error	t value	$Pr(>\|t\|)$
$f_{0,0}$	249.6	2.624×10^{-3}	95096.64	$< 2 \times 10^{-16}$
$f_{1,0}$	-0.9889	7.132×10^{-5}	-13865.51	$< 2 \times 10^{-16}$
$f_{0,1}$	1.074	4.593×10^{-4}	2338.70	$< 2 \times 10^{-16}$
$f_{2,0}$	-6.566×10^{-3}	4.676×10^{-6}	-1404.23	$< 2 \times 10^{-16}$
$f_{1,1}$	1.148×10^{-2}	2.410×10^{-5}	476.27	$< 2 \times 10^{-16}$
$f_{0,2}$	-5.947×10^{-3}	1.814×10^{-4}	-32.79	$< 2 \times 10^{-16}$

Table 1: Statistical analysis for regression method for approximating iteration map H_1^p for $p = 2$. There are 1000 data points, 6 unknown coefficients $f_{\alpha\beta}$'s, and 994 degrees of freedom. The residual standard error is 0.04221. Robustness is assured by the following statistical criteria: multiple R-squared is 1, adjusted R-squared is 1, the F-statistic value is 4.04×10^7 on 5 and 994 degrees of freedom, and the p-value is below 2.2×10^{-16}.

p	ℓ	RSS	RSE
2	6	1.771	0.04221
3	10	1.639	0.04069
4	15	0.2382	0.01555
5	21	0.1986	0.01424
6	28	0.1975	0.01425
7	36	0.1963	0.01427

Table 2: Values of ℓ, RSS and RSE for the approximate function H_1^p of different order p for Tolkacheva et al.'s model.

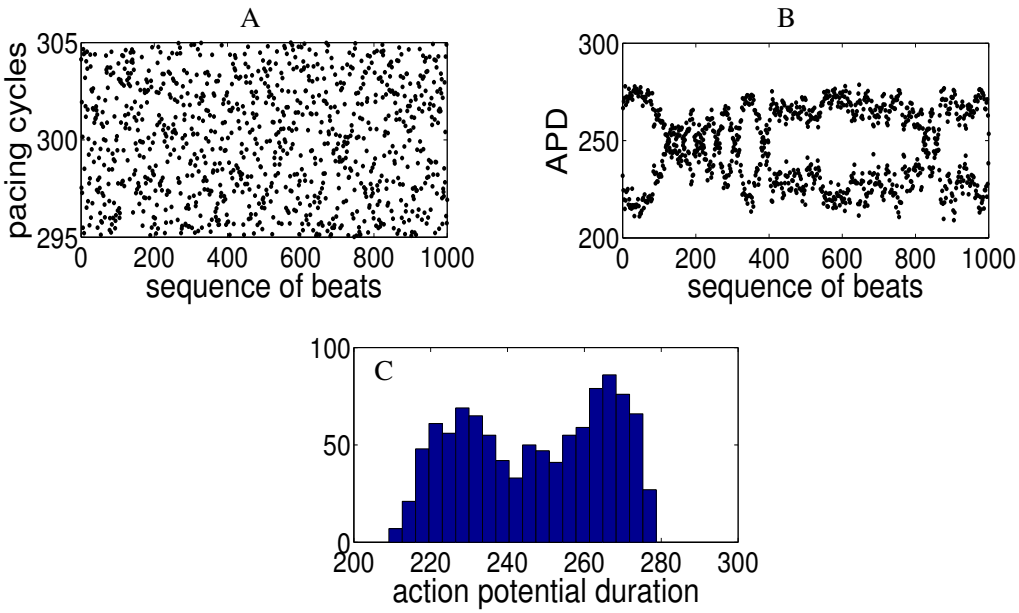

Figure 4: A) sequence of pacing cycles; B) sequence of corresponding APDs; C) histogram of all APDs.

It is obvious that for larger order p, the approximation becomes more accurate. However, there are also more undetermined coefficients $f'_{\alpha\beta}s$ in (2.8). Let $\ell = \ell(k,p)$ be the number of the undetermined coefficients $f_{\alpha\beta}$ in H_k^p in (2.8) where $k = 1$ indicates dependence on only the most recent stimulus interval T_{n-1}.

Two statistical values are significant to judge the accuracy of the approximation: RSS (residual sum of the squares)

$$R_{ss} = \sum \left(A_n - H_1^p(D_{n-1}, A_{n-1})\right)^2, \tag{2.10}$$

and RSE (residual standard error)

$$r_{se} = \sqrt{\frac{R_{ss}}{N-\ell}}. \tag{2.11}$$

As we increase the order of the approximate function H_1^p, the RSS and RSE both decrease, but ℓ increases. Table 2 shows the values of ℓ, RSS and RSE for different orders p. Notice that as p increases from 2 to 5, there is a significant decrease in both RSS and RSE, however, there is very little improvement as p is increased further, even though the number of parameters increases substantially. Therefore, it appears that $p = 5$ is in some heuristic sense "optimal". In the next section, we provide a less heuristic criterion to determine the "best" fit.

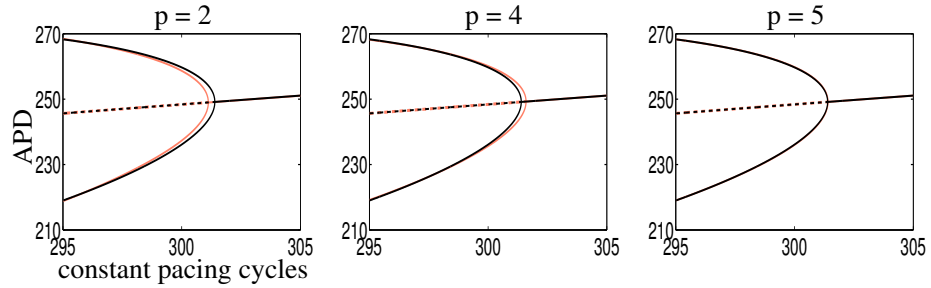

Figure 5: (Color online) Comparison of the bifurcation diagrams between the theoretical map (A.1) (black) and approximate form (2.8) (red, light grey) for various orders of p. The solid curve indicates stability and dashed curve indicates instability. Note that for all cases the approximate fixed points are very close to the theory and they are not distinguishable in the graph. In addition, for the case $p = 5$, the theoretical and approximate diagrams almost coincide.

3 Approximate Fox et al.'s Model: An Example of Mapping Model With One Memory Variable

The mapping model with one memory variable in the following form

$$\begin{cases} A_n = f(D_{n-1}, M_n), \\ M_n = g(A_{n-1}, M_{n-1}, T_{n-1}), \\ D_n = T_n - A_n \end{cases} \tag{3.1}$$

is regarded as a good approximation for the behavior of quite a few ionic models [8, 14, 15, 18]. A specific example of (3.1) is the model by Fox et al. [15], which is described in detail in (A.5).

We start with the model (3.1). Some expanded forms of (3.1) were considered by previous researchers. For instance, in [25] the authors proposed that

$$A_n = f(D_{n-1}, A_{n-1}, D_{n-2}, A_{n-2}, \ldots)$$

and analyzed the different restitution curves in the restitution portrait [26]. However, to best apply our method, we need a different form which is more "compact". If we substitute the memory terms M_k of the second equation into the first equation in (3.1) for $k = n, n-1, \ldots$, we may write

$$A_n = F_n(A_0, M_0; A_{n-1}, A_{n-2}, \ldots, A_1; T_{n-1}, T_{n-2}, \ldots, T_0), \tag{3.2}$$

using that $D_n = T_n - A_n$. The function F_n in (3.2) is some combination of compositions of f and g, and A_0 and M_0 are initial values. We note that the functions F_n are different for each n. We

call (3.2) the expansion form of the mapping model (3.1). If we substitute the equation (3.2) for A_{n-2}, A_{n-3}, ... into the equation for A_n, we may rewrite (3.2) as

$$A_n = \widetilde{F}_n(A_0, M_0, A_{n-1}; T_{n-1}, T_{n-2}, \ldots, T_0), \tag{3.3}$$

for some function $\widetilde{F}_n$, which also depends on n.

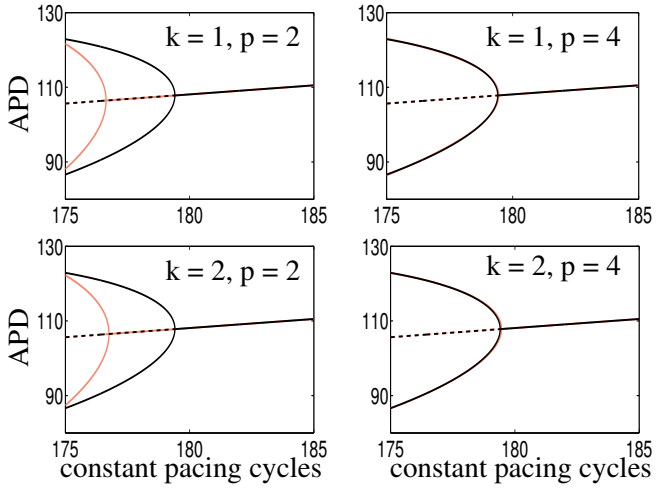

Figure 6: (Color online) Comparison of the bifurcation diagrams between the theoretical map (3.1) (black) and approximate form (3.5) (red, light grey) for various values of k and p. The solid line indicates stability and dashed line indicates instability. We note that in each of the two cases $(k, p) = (1, 4)$ and $(2, 4)$, the dynamics of theory and the approximation are very close and their bifurcation diagrams almost coincide.

In the long time run, one would expect that the information of the distant past should have little impact on current APD, which suggests that we make the following approximation: for sufficiently large n, there are iterative maps H_k's in the following form, for $k = 1, 2, \ldots$,

$$A_n \sim H_k(A_{n-1}; T_{n-1}, T_{n-2}, \ldots, T_{n-k}), \tag{3.4}$$

which approximates the dynamics of (1.2), i.e., the function H_k is some approximation which only includes the most recent k memories. That this approximation is valid remains a conjecture, although a rigorous proof can be given for some particular models, for example, the model proposed by Schaeffer et al. [18], in which the memory M_n only depends on A_{n-1} and T_{n-1}. It is obvious that for larger k, the approximation cannot be less accurate.

The analytical form of the function H_k is unknown in general, however, H_k may be approximated

by some polynomial $H_k^p(A_{n-1}; T_{n-1}, T_{n-2}, \ldots, T_{n-k})$ for $k \geq 0$ and $p \geq 2$ in the following form,

$$\begin{aligned} A_n &\sim H_k^p(A_{n-1}; T_{n-1}, T_{n-2}, \ldots, T_{n-k}) \\ &= \sum h_{\alpha\beta_1\beta_2\ldots\beta_k}(A_{n-1} - \bar{A})^\alpha (T_{n-1} - \bar{T})^{\beta_1}(T_{n-2} - \bar{T})^{\beta_2} \ldots (T_{n-k} - \bar{T})^{\beta_k}, \end{aligned} \tag{3.5}$$

where k denotes that the approximation involves information from previous k beats, p is the order of approximate polynomial, and the summation is taken over the nonnegative indices $\alpha+\beta_1+\ldots+\beta_k \leq p$.

Now to approximate H_k^p we assume that the pacing cycles $T_n's$ are random and with some random initial value, we generate $N = 1000$ data points for the sequence of A_n's using Fox et al.'s model (A.5). We also add a noise term $\epsilon\xi_n$ to each A_n as in (2.9) to mimic the error in measuring APDs, with $\epsilon = 0.01$ms. Then given a set of data groups $(A_n, A_{n-1}, T_{n-1}, \ldots, T_{n-k})$, we use the regression method to estimate the best choice of the unknown coefficients $h_{\alpha\beta_1\beta_2\ldots\beta_k}$ to obtain the approximate form (3.5). We then compare the bifurcation diagrams of the original Fox et al.'s model (A.5) and of the approximate form (3.5), shown in Figure 6 for several values of k and p.

Notice that for larger k and p, the approximation is increasingly accurate (as expected). However, the total number of unknown coefficients, $\ell(k, p)$ also becomes larger. Therefore, the "optimal" parameter choice should in some way minimize the error as well as the number of unknown coefficients. One useful way to determine the best parameter set is to minimize the Bayesian information criterion (BIC) function [27],

$$B(k, p) = N \log\left(\frac{R_{ss}}{N}\right) + \ell(k, p)\log(N), \tag{3.6}$$

where R_{ss} is the RSS defined in (2.10).

In Table 3 we show RSS, RSE and BIC values for several cases of (k, p), and Figure 7 shows the RSE and BIC versus p for different values of k. Once again, we see that the RSE decreases rapidly until $p = 4$, but there is very little improvement for larger values of p. Also, the BIC decreases as p increases to 4, but then increases for larger values of p, due to the fact that RSE is decreasing slowly while $\ell(k, p)$ is increasing rapidly as a function of p. Since BIC is minimized at $k = 2$ and $p = 4$, we take the polynomial $H_{2,4}(A_{n-1}; T_{n-1}, T_{n-2})$, i.e.,

$$\begin{aligned} A_n &\sim H_{2,4}(A_{n-1}; T_{n-1}, T_{n-2}) \\ &= \sum_{0\leq\alpha+\beta_1+\beta_2\leq 4} h_{\alpha\beta_1\beta_2}(A_{n-1} - \bar{A})^\alpha (T_{n-1} - \bar{T})^{\beta_1}(T_{n-2} - \bar{T})^{\beta_2}, \end{aligned} \tag{3.7}$$

where the coefficients $h_{\alpha\beta_1\beta_2}$'s are determined by the regression method to be the "best" approximation of Fox et al.'s model.

Now we come back to the model by Tolkacheva et al. discussed in Section 2. We assume that the model is in the general form (3.1), and repeat the previous process for different values of (k, p). We show the results for some significant cases of (k, p) in Table 3. Notice that the choice of (k, p) that minimizes the BIC is $(1, 5)$.

k	p	$\ell(k,p)$	RSS	RSE	BIC	k	p	$\ell(k,p)$	RSS	RSE	BIC
0	2	3	11.36	0.1067	-4457	3	2	15	8.317	0.09189	-4686
0	3	4	3.51	0.05936	-5625	3	3	35	1.426	0.03844	-6311
0	4	5	1.941	0.04417	-6210	3	4	70	0.1829	0.01402	-8123
0	5	6	1.937	0.04415	-6205	3	5	126	0.1631	0.01366	-7851
⋮	⋮	⋮	⋮	⋮	⋮	3	6	210	0.151	0.01383	-7348
1	2	6	8.615	0.0931	-4713	⋮	⋮	⋮	⋮	⋮	⋮
1	3	10	1.635	0.04064	-6347	4	2	21	8.176	0.09139	-4662
1	4	15	0.242	0.01568	-8223	4	3	56	1.342	0.0377	-6227
1	5	21	0.2247	0.01515	-8256	4	4	126	0.1734	0.01409	-7790
1	6	28	0.2225	0.01513	-8217	4	5	252	0.1453	0.01394	-7096
⋮	⋮	⋮	⋮	⋮	⋮	⋮	⋮	⋮	⋮	⋮	⋮
2	2	10	8.491	0.09261	-4700	5	2	28	7.887	0.09008	-4649
2	3	20	1.523	0.03942	-6349	5	3	84	1.278	0.03735	-6082
2	**4**	**35**	**0.1906**	**0.01405**	**-8323**	5	4	210	0.1587	0.01418	-7298
2	5	56	0.1734	0.01355	-8273	5	5	462	0.1077	0.01415	-5945
2	6	84	0.1678	0.01354	-8112	⋮	⋮	⋮	⋮	⋮	⋮
⋮	⋮	⋮	⋮	⋮	⋮	10	2	78	7.058	0.08749	-4415
						10	3	364	0.8494	0.03655	-4557

Table 3: RSS, RSE and BIC values of the approximate function H_k^p for Fox et al.'s model for some significant cases of (k,p) pairs, where $k \geq 0$, $p \geq 2$ and $\ell(k,p) < N/2$.

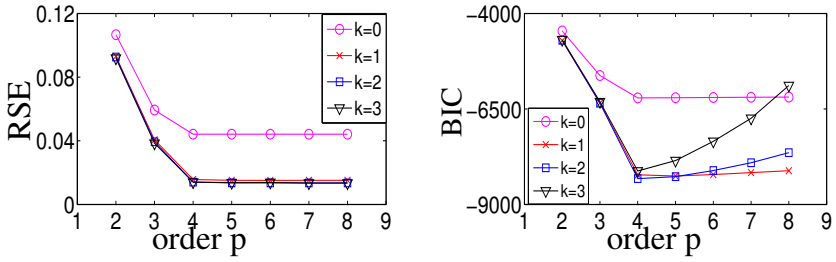

Figure 7: (Color online) Approximate the model of Fox et al.: RSE and BIC values of each polynomial H_k^p versus p for $k = 0, 1, 2, 3$.

k	p	$\ell(k,p)$	RSS	RSE	BIC
0	3	4	65.78	0.257	-2694
0	4	5	63.34	0.2523	-2725
⋮	⋮	⋮	⋮	⋮	
1	3	10	1.639	0.04069	-6344
1	4	15	0.2382	0.01555	-8239
1	**5**	**21**	**0.1986**	**0.01424**	**-8379**
1	6	28	0.1975	0.01425	-8337
⋮	⋮	⋮	⋮	⋮	
2	4	35	0.2284	0.01538	-8143
2	5	56	0.1889	0.01415	-8188
2	6	84	0.1857	0.01424	-8011

Table 4: RSS, RSE and BIC values of the approximate function H_k^p for Tolkacheva et al.'s model for some significant cases of (k, p) pairs. The best choice of (k, p) is $(1, 5)$.

4 General Mapping Model with Multiple Memory Variables

For the most general mapping model with multiple memory variables (1.2), i.e., $J > 1$, the approach is similar to the case with only one memory variable. For each memory variable $M_n^{(j)}$, we substitute the second equation into the first equation of (1.2) recursively for $n-1$, $n-2$, …, 2, 1, to obtain the relationship

$$A_n = F_n(A_0; M_0^{(1)}, M_0^{(2)}, \ldots, M_0^{(J)}; A_{n-1}, A_{n-2}, \ldots, A_1; T_{n-1}, T_{n-2}, \ldots, T_0).$$

Following a similar argument as above, we assume that in the long time run, i.e., when n is sufficiently large, this function can be approximated by a polynomial H_k^p in the same form as (3.5),

with k memories and polynomial of degree p. We apply the same methodology as in Section 3: we determine the unknown coefficients $h_{\alpha\beta_1\beta_2\ldots\beta_k}$ using regression, and compute the RSS, RSE and BIC values for each (k,p). We then obtain the optimal choice of (k,p) by minimizing the BIC value.

5 Discussion

For a general mapping model (1.2), we assume there are iterative maps H_k's in (3.4) and approximate each H_k by the polynomial H_k^p in (3.5) for various orders p. A necessary condition for the existence of H_k's is that the coefficients of H_k^p's obtained by the regression method have the following consistency property: the coefficient for the same term is close in each H_k^p, or it has some tendency of convergence as k and p become larger. For example, we expect that $h_{1,0,\ldots,0}$, the coefficient of $(A_{n-1}-\bar{A})$ in each H_k^p, should not vary much as $k,p\to\infty$. In Figure 8, we show the values of the coefficients of $(A_{n-1}-\bar{A})$ and $(A_{n-1}-\bar{A})(T_{n-1}-\bar{T})$ versus p for different values of k for the Fox et al. model described in Section 3. Consistency can be observed in each coefficient.

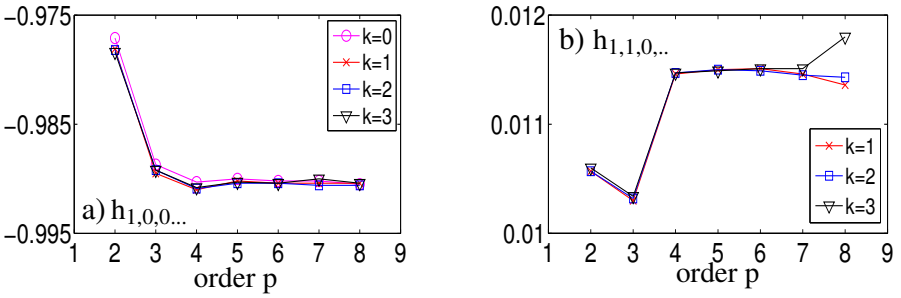

Figure 8: (Color online) (a) the value of $h_{1,0,0,\ldots}$, the coefficient for $(A_{n-1}-\bar{A})$ versus the order p for different values of k; (b) the value of $h_{1,1,0,\ldots}$, the coefficient for $(A_{n-1}-\bar{A})(T_{n-1}-\bar{T})$ versus the order p for different values of k.

The role of ϵ in (2.9) is important. When ϵ is small, earlier memories are able to be detected and higher order accuracy can be obtained; when ϵ is large, the noise in the measurement may mask the memory so that it cannot be detected. For the model of Fox et al. discussed in Section 3, if $\epsilon=10^{-4}$, we find that $k=3$ and $p=6$ is optimal, while if $\epsilon=0.1$, we find that $k=1$ and $p=4$ is optimal. In Figure 9(a-d) we show the RSE and BIC versus p for various k for each case respectively. We also show bifurcation diagrams at the optimal choice of (k,p) for each case in Figure 9(e,f), compared to the theoretical bifurcation diagrams. It is not surprising that a better approximation can be obtained with less noise.

The number of data points N is also important. Roughly speaking, if there are more data points for a fixed time interval, we can obtain better accuracy of the approximate dynamics. Table 5 shows

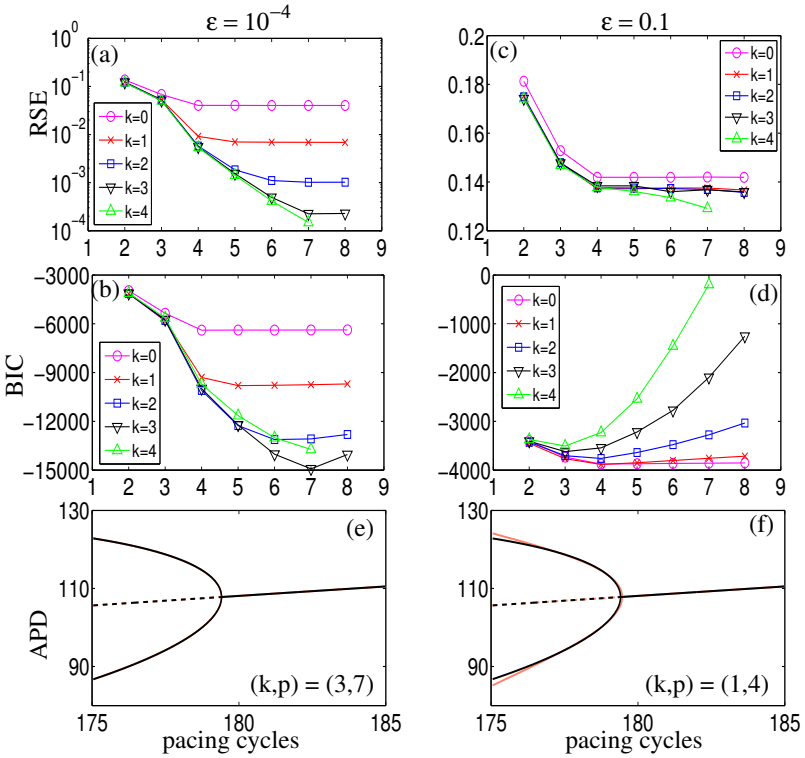

Figure 9: (Color online) The RSE and BIC values of the approximate polynomial H_k^p versus the order p for various k, and bifurcation diagrams of H_k^p at optimal choice of (k, p) for different measurement error $\epsilon = 10^{-4}$ (a, c, e) and $\epsilon = 0.1$ (b, d, f) respectively for Fox et al.'s model. In (e) and (f), the theoretical bifurcation diagram (black) and the approximation (red, light grey) are drawn for comparison, and in (e) the theory and approxmation almost coincide.

the optimal choice of (k, p) and the corresponding RSE for a variety of N. In Figure 10 we show the bifurcation diagrams of the optimal approximate H_k^p for various ϵ and N. Clearly, for larger measurement error (ϵ), more data points (N) are needed in order to ensure a good approximate bifurcation curve.

The method we described here does not require any particular distribution for the stochastic pacing cycles T_n's, although in Section 2 and 3, we used the uniform distribution as an example. We tested some other distributions. In Figure 11 we show the results for some other distributions of pacing cycles, where we use the Fox et al. model with testing time interval $[\mu_a, \mu_b] = [175, 185]$, number of data points $N = 1000$ and $\epsilon = 0.01$. We find that in each case, our method gives reliable results, although the best choice of k and p can differ.

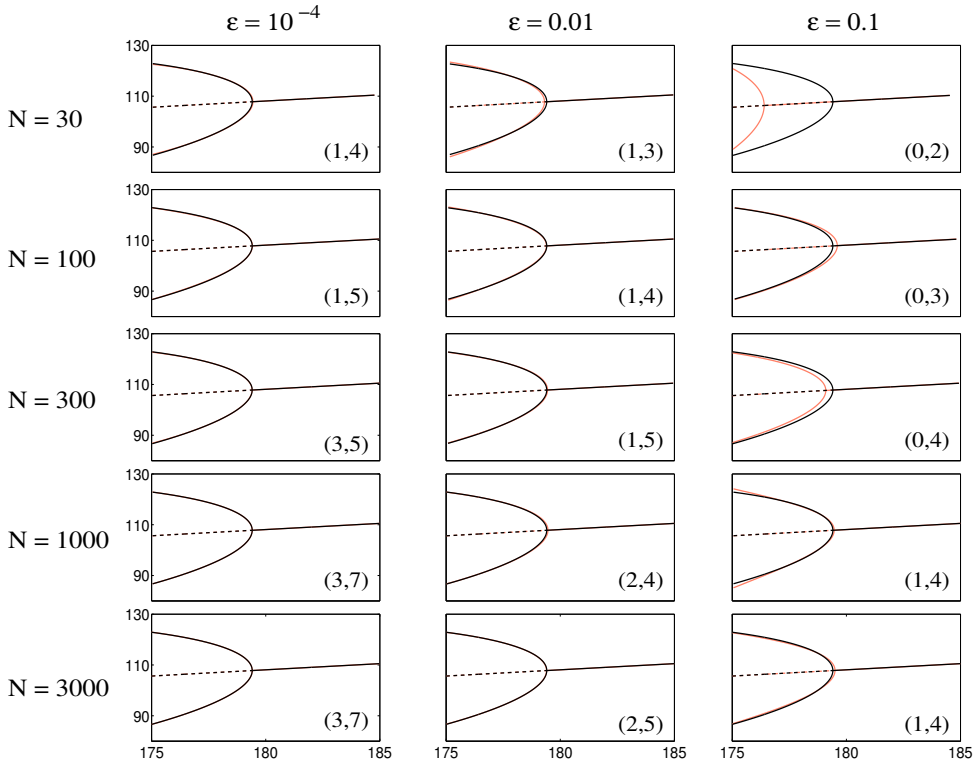

Figure 10: (Color online) Bifurcation diagrams of the optimal approximate H_k^p (red, light grey) compared to the exact result (black) for various values of ϵ and N. In some subpictures the approximate and exact diagrams almost coincide. The corresponding optimal choice of (k, p) is shown in the right-bottom corner of each subpicture.

Although our method is based on a discussion on small variation in pacing cycles, exciting results are obtained when the method is applied to larger regions of pacing cycles. In Figure 12 we show the results for different time intervals $[\mu_a, \mu_b] = [160, 200], [130, 170], [90, 190]$ for $\epsilon = 0.01$ and 0.1 respectively, and the approximation matches the theory quite well in each case.

6 Conclusion

In this paper, we provide a new approach to investigate APD restitution and bifurcations when there is memory. We use stochastic pacing cycles to simulate the model to obtain the data (a series of APDs) and we find an approximate polynomial using a regression method. We are then able to produce bifurcation diagrams corresponding to the approximate restitution function. We demonstrate the process with data generated by the models of Tolkacheva et al. and Fox et al. The

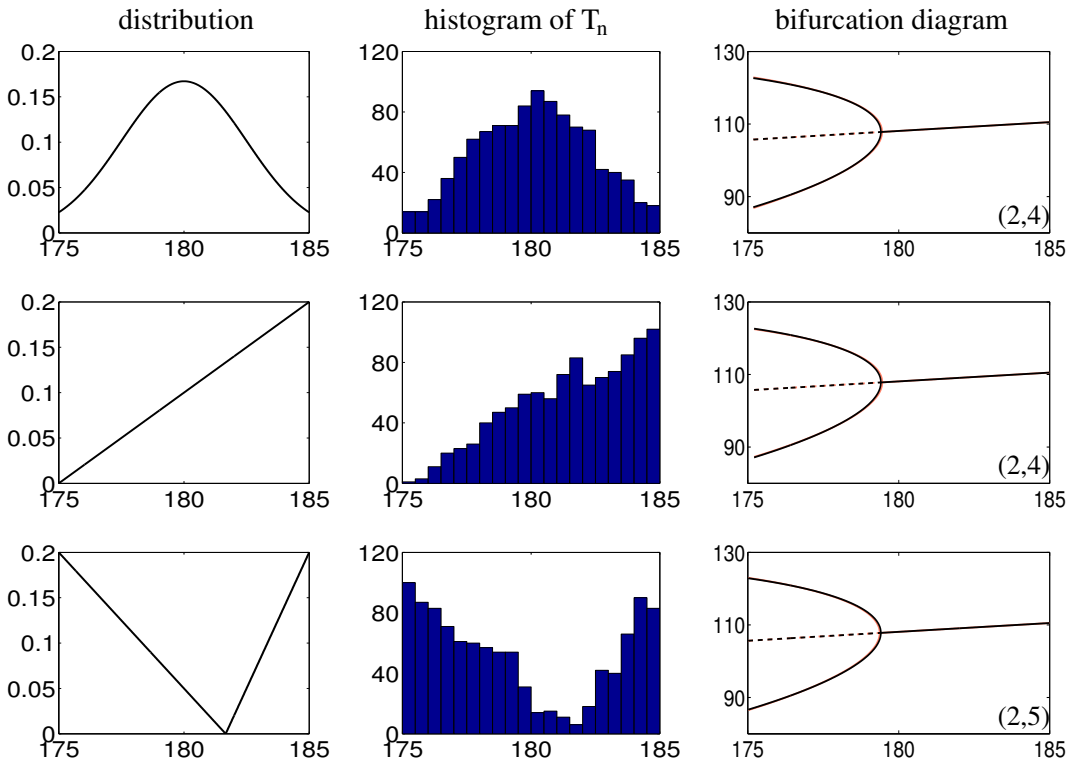

Figure 11: (Color online) Probability density function and histogram of the applied pacing cycles, and bifurcation diagram of the optimal approximate H_k^p (red, light grey) compared to the exact curve (black) for three different distributions of pacing cycles, where $N = 1000$ and $\epsilon = 0.01$. Optimal choice of (k, p) is labelled in each picture of bifurcation diagram. We note that the approximate and the exact bifurcation diagrams are very close and hard to distinguish in all the pictures.

procedure is summarized as follows: 1) First, generate a random series of pacing cycles in a time interval of interest from some distribution. 2) Apply stimuli with this pacing protocol and record the corresponding APDs. 3) Compute $\bar{T}$ and $\bar{A}$, the sample mean of the pacing cycles and APDs respectively and then for each (k, p) find a polynomial in the form (3.5) by regression and obtain the RSS and RSE values. 5) Compute the BIC value for each approximation and determine the optimal (k, p) which has minimal BIC value. 6) Use the corresponding polynomial H_k^p to approximate the dynamics and determine the bifurcation structure.

The method of stochastic pacing we introduce here has several advantages over previous protocols: 1) The pacing protocol is simple, as we only need to generate a few hundred pacing cycles, 2) the approximate dynamics are obtained in an entire time interval of interest, not merely at a single

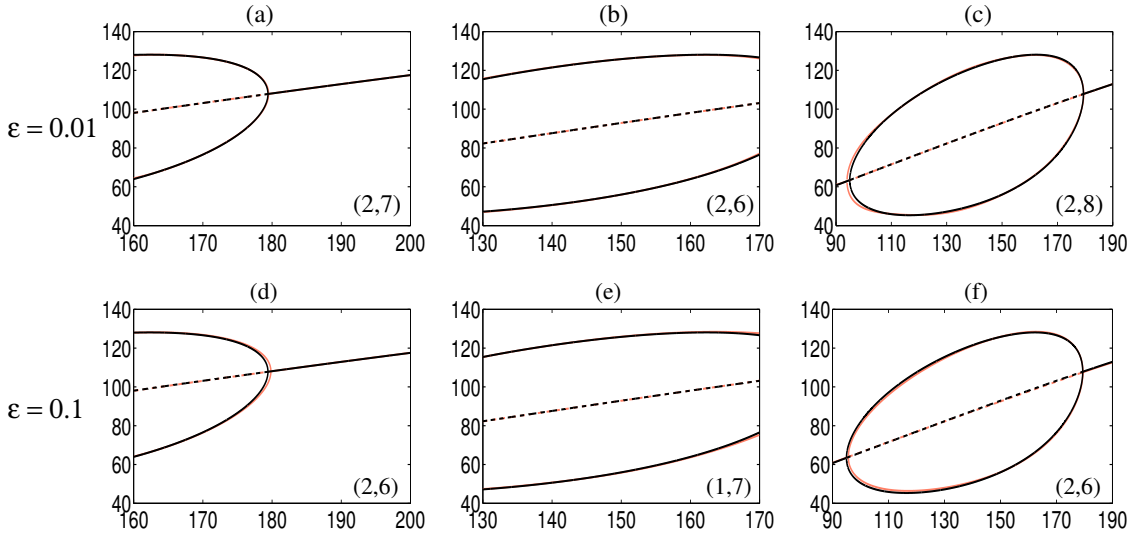

Figure 12: Bifurcation diagrams of the optimal approximate H_k^p (red, light grey) compared to the exact result (black) for various testing time intervals, for $\epsilon = 0.01$ (a, b, c) and 0.1 (d, e, f) respectively, and in all cases $N = 1000$. In some subpictures the approximate and exact diagrams almost coincide. Optimal choice of (k, p) is shown in the right-bottom corner of each subpicture.

point, 3) we are able to deal with cases when the fixed point is unstable and alternans appears, thereby detecting bifurcations, 4) we have high order of accuracy.

While we illustrated this method using data from specific models, one could also generate the data using full ionic models, or directly from in vitro experiments. We also expect that this method can be used to analyse data from in vivo experiments. In vivo, the pacing protocol is not externally generated but because it is variable, the same ideas can be applied. In future work, we will use this method to study several important ionic models.

Acknowledgments

We would like to thank the referees and the editor for their very valuable comments and suggestions. This work is under the support of the National Science Foundation under agreement 0635561, NSF-DMS-0931642, NSF-DMS-0718036 and NSF-DMS-1122297.

	$\epsilon = 10^{-4}$		$\epsilon = 0.01$		$\epsilon = 0.1$	
N	optimal (k,p)	RSE	optimal (k,p)	RSE	optimal (k,p)	RSE
30	(1,4)	0.005963	(1,3)	0.01691	(0,2)	0.1299
100	(1,5)	0.006378	(1,4)	0.01644	(0,3)	0.1389
300	(3,5)	0.000235	(1,5)	0.01642	(0,4)	0.1385
1000	(3,7)	0.000225	(2,4)	0.01405	(1,4)	0.1372
3000	(3,7)	0.000228	(2,5)	0.01419	(1,4)	0.1414

Table 5: Optimal choice of (k,p) and corresponding RSE versus different number of data points N and measurement error ϵ. We are able to detect earlier memory and achieve better accuracy if we have more data points or lower measurement error.

Appendix

I. Tolkacheva et al.'s Model

The mapping model of Tolkacheva et al. [16] is in the form

$$\widetilde{A}_{n+1} = f(\widetilde{A}_n, \widetilde{D}_n) = C_1 - \frac{r_{\text{cur}}}{P(\widetilde{A}_n, \widetilde{D}_n)} + \sqrt{1 - \frac{C_2}{P(\widetilde{A}_n, \widetilde{D}_n)} + \left[\frac{r_{\text{cur}}}{P(\widetilde{A}_n, \widetilde{D}_n)}\right]^2}, \tag{A.1}$$

where $\widetilde{A}_n = A_n/\tau_{\text{sclose}}$ and $\widetilde{D}_n = D_n/\tau_{\text{sclose}}$ are dimensionless variables, and

$$P(\widetilde{A}, \widetilde{D}) = 1 - \left(1 - G(\widetilde{A})e^{-\widetilde{A}}\right) e^{-D\ r_{\text{gate}}} \tag{A.2}$$

$$G(\widetilde{A}) = \frac{r_{\text{cur}}\widetilde{A} - (1 - v_{\text{crit}})r_{\text{mix}}}{1 - \exp(-\widetilde{A} + r_{\text{mix}}(v_{\text{sig}} - v_{\text{crit}})/r_{\text{cur}})} \tag{A.3}$$

with the constants

$$C_1 = 1 + \frac{r_{\text{mix}}}{r_{\text{cur}}}(v_{\text{sig}} - v_{\text{crit}}), \quad C_2 = 2[r_{\text{cur}} + r_{\text{mix}}(v_{\text{sig}} - 1)]. \tag{A.4}$$

Typical values of the parameters are listed in Table 6

II. Fox et al.'s model

The mapping model by Fox et al. [15] is in the following form,

$$\begin{cases} A_n = f(D_{n-1}, M_n), \\ M_n = g(M_{n-1}, D_{n-1}, A_{n-1}), \\ D_n = T_n - A_n, \end{cases} \tag{A.5}$$

Parameter	Value (ms)	Parameter	Value (dimensionless)
τ_{sclose}	1000	v_{crit}	0.13
τ_{slow}	127	v_{sig}	0.85
τ_{ung}	130	κ	40
τ_{sopen}	50	v_{vout}	0.1
τ_{fopen}	18		
τ_{fclose}	10		
τ_{fast}	0.25		

Table 6: Typical parameter values in Tolkacheva et al.'s model.

where

$$f(D, M) = (1 - c_0 M)\left(c_1 + \frac{c_2}{1 + e^{-(D-c_3)/c_4}}\right), \tag{A.6}$$

$$g(M, D, A) = e^{-D/\tau}\left(1 + (M-1)e^{-A/\tau}\right). \tag{A.7}$$

Typical values for the parameters are given in Table 7.

Parameter	Value	Units
c_0	0.9	dimensionless
c_1	88	ms
c_2	122	ms
c_3	40	ms
c_4	23	ms
τ	160	ms

Table 7: Typical parameter values in Fox et al.'s model.

References

[1] D. Noble, *A modification of the Hodgkin-Huxley equations applicable to Purkinje fibre action and pacemaker potential*, J. Physiol. 160(1962) 317-352.

[2] G. W. Beeler and H. Reuter, *Reconstruction of the action potential of ventricular myocardial fibers*, J. Physiol. 268(1977) 177-210.

[3] C. H. Luo and Y. Rudy, *A dynamic model of the cardiac ventricular action potential. I. Simulations of ionic currents and concentration changes*, Circ. Res. 74(1994): 1071-1096.

[4] V. Iyer, R. Mazhari1 and R. L. Winslow, *A computational model of the human left-ventricular epicardial myocyte*, Biophys. J. 87(2004) 1507-1525.

[5] A. Mahajan, Y. Shiferaw, D. Sato, A. Baher, R. Olcese, L. H. Xie, M. J. Yan, P. S. Chen, J. G. Restrepo, A. Karma, A. Garfinkel, Z. Qu and J. N. Weiss, *A rabbit ventricular action potential model replicating cardiac dynamics at rapid heart rates*, Biophys. J. 94(2008) 392-410.

[6] J. B. Nolasco and R. W. Dahlen, *A graphic method for the study of alternation in cardiac action potentials*, J. Appl. Physiol. 25(1968) 191-196.

[7] M. Guevara, G. Ward, A. Shrier and L. Glass, *Electrical alternans and period-doubling bifurcations*, IEEE Comp. Cardiol. 562(1984) 167-170.

[8] D. R. Chialvo, D. C. Michaels and J. Jalife, *Supernormal excitability as a mechanism of chaotic dynamics of activation in cardiac Purkinje fiber*, Circ. Res. 66(1990) 525-545.

[9] N. F. Otani and R. F. Gilmour, *Memory models for the electrical properties of local cardiac systems*, J. Theor. Biol. 187(1997)409-436.

[10] R. F. Gilmour, N. F. Otani, and M. A. Watanabe, *Memory and complex dynamics in cardiac Purkinje fibers*, Am. J. Physiol. Heart Circ. Physiol. 272(1997) H1826-H1832.

[11] G. M. Hall, S. Bahar, and D. J. Gauthier, *Prevalence of rate-dependent behaviors in cardiac muscle*, Phys. Rev. Lett. 82(1999) 2995-2998.

[12] W. A. Watanabe and M. L. Koller, *Mathematical analysis of dynamics of cardiac memory and accommodation: theory and experiment*, Am. J. Physiol. Heart Circ. Physiol. 282(2002) H1534-1547.

[13] E. Cytrynbaum and J. P. Keener, *Stability conditions for the traveling pulse: Modifying the restitution hypothesis*, Chaos 12(2002) 788-799.

[14] E. G. Tolkacheva, D. G. Schaeffer, D. J. Gauthier and C. C. Mitchell, *Analysis of the Fenton-Karma model through an approximation by a one-dimensional map*, Chaos 12(2002) 1034-1043.

[15] J. J. Fox, E. Bodenschatz and R. F. Gilmour, Jr., *Period-Doubling Instability and Memory in Cardiac Tissue*, Phys. Rev. Lett. 89(2002) 138101.

[16] E. G. Tolkacheva, D. G. Schaeffer, D. J. Gauthier and W. Krassowska, *Conditions for alternans and stability of the 1:1 response pattern in a "memeory" model of paced cardiac dynamics*, Phys. Rev. E, 67(2003) 031904.

[17] Y. Shiferaw, Z. Qu, A. Garfinkel, A. Karma and J. N. Weiss, *Nonlinear dynamics of paced cardiac cells*, Ann. N.Y. Acad. Sci. 1080(2006) 376-394 .

[18] D. G. Schaeffer, J. W. Cain, D. J. Gauthier, S. S. Kalb, R. A. Oliver, E. G. Tolkacheva, W. Ying and W. Krassowska, *An ionically based mapping model with memory for cardiac restitution*, Bull. Math. Biol. 69(2007), 459-482.

[19] Z. Qu, Y. Shiferaw and J. N. Weiss, *Nonlinear dynamics of cardiac excitation-contraction coupling: An iterated map study*, Phys. Rev. E 75(2007) 011927.

[20] T. Kuusela, *Stochastic heart-rate model can reveal pathologic cardiac dynamics*, Phys. Rev. E 69(2004), 031916.

[21] C. Lerma,T. Krogh-Madsen, M. Guevara1 and L. Glass, *Stochastic aspects of cardiac arrhythmias*, J. Stat. Phys. 128(2007) 347-374.

[22] N. Karim, J. A. Hasan and S. S. Ali, *Heart rate variability – a review*, J. Basic Appl. Sci., 7(2011), 71-77.

[23] L. A. N. Amaral, A. L. Goldberg, P. C. Ivanov and H. E. Stanley, *Modeling heart rate variability by stochastic feedback*, Comp. Phys. Commun. 121-122(1999) 126-128.

[24] D. C. Trost, *A Method for constructing and estimating the RR-memory of the QT-interval and its inclusion in a multivariate biomarker for torsades de pointes risk*, J. Biopharm. Stat. 18(2008), 773-796.

[25] S. S. Kalb, E. G. Tolkacheva, D. G. Schaeffer, D. J. Gauthier, and W. Krassowska, *Restitution in mapping models with an arbitrary amount of memory*, Chaos 15(2005) 023701.

[26] S. S. Kalb, H. M. Dobrovolny, E. G. Tolkacheva, S. F. Idriss, W. Krassowska and D. J. Gauthier, *The restitution portrait: a new method for investigating rate-dependent restitution*, J. Cardiovasc. Electrophysiol. 15(2004) 698-709.

[27] G. E. Schwarz, *Estimating the dimension of a model*, Ann. Statist. 6(1978), 461-464.